

## Atomistic Mechanisms of Fatigue in Nanocrystalline Metals

D. Farkas,\* M. Willemann, and B. Hyde

*Department of Materials Science and Engineering, Virginia Polytechnic Institute and State University,  
Blacksburg, Virginia 24061, USA*

(Received 18 October 2004; published 26 April 2005)

We investigate the mechanisms of fatigue behavior in nanocrystalline metals at the atomic scale using empirical force laws and molecular level simulations. A combination of molecular statics and molecular dynamics was used to deal with the time scale limitations of molecular dynamics. We show that the main atomistic mechanism of fatigue crack propagation in these materials is the formation of nanovoids ahead of the main crack. The results obtained for crack advance as a function of stress intensity amplitude are consistent with experimental studies and a Paris law exponent of about 2.

DOI: 10.1103/PhysRevLett.94.165502

PACS numbers: 62.20.Mk, 62.25.+g

*Introduction.*—Fatigue of metallic materials is an important issue in the field of mechanical behavior. Nanocrystalline materials are especially susceptible to fatigue failure [1,2]. This behavior is attributed to the large volume fraction of grain boundary material. The details of fatigue failure and the mechanisms by which it occurs are not well understood. Theoretical models have generally been limited to the macroscopic and mesoscales, and no studies have been performed at the atomistic level to the best of our knowledge [3–6]. The two basic reasons why fatigue has not been studied atomistically relate to the length and time scales. In this Letter we show that with current computing power we can approach the experimental fatigue length scale of nm/cycle crack extension. The key issue of MD time scale (ns) vs experimental fatigue time scale(s) is addressed in the present work using a combination of molecular statics and molecular dynamics. The combined results of these two techniques are shown to allow basic understanding of the essential processes of crack advance under cyclic loading.

The simulations we present here utilize an embedded-atom method (EAM) potential for Ni that is based on first principle calculations [7] and has been tested as part of our previous work dealing with fracture under monotonic loading [8]. In this Letter, we report the first simulations under cyclic loading performed on a digital sample with a columnar grain structure with random misorientations and a 6 nm grain size. We demonstrate that we can reach the Paris regime, and we analyze the detailed mechanism of fatigue crack advance in nanocrystalline materials.

*Simulation technique.*—The simulation of fracture is performed introducing a semi-infinite crack loaded to a given stress intensity  $K$ . In both molecular dynamics and molecular statics the loading is introduced by using displacement fields obtained from the elasticity theory for the given value of the stress intensity. The introduction of the crack is also performed using continuum solutions based on the linear elasticity theory. The role of the continuum solution is twofold. First, it serves as an initial guess for the relaxed atomic configuration in all the regions of the

simulation. Second, it serves as boundary conditions that are kept fixed in the regions far from the crack tip. Based on continuum fracture mechanics, the elastic solution should be valid far from the crack tip. The atomic positions far from the crack tip are held fixed according to the elastic solution during the conjugate gradient routine used in molecular statics or during a certain number of time steps in the molecular dynamics technique. As the simulation proceeds, the loading can be increased or decreased superposing corresponding displacement given by linear elasticity, updating the fixed boundary conditions to those representative of a crack with a higher or a lower loading level. These displacements can be used to simulate cyclic loading by applying a load to a certain stress intensity  $K_{\max}$  for the first part of the cycle and then superposing displacements corresponding to reach a lower stress intensity  $K_{\min}$  in the second part of the cycle. The cyclic process between maximum and minimum stress intensities can be simulated with either molecular dynamics or molecular statics. The latter technique simulates an equilibrium configuration in the crack tip area at both the minimum and maximum loading points of each cycle. Alternatively, molecular dynamics represents the response of the crack tip at extremely high cycling rates. In the work reported here we used both techniques.

The initial atomic configurations used in our studies were generated using a Voronoi construction [9]. The columnar grains in the sample were generated by using a common [110] axis for all grains and a random rotation angle around this axis for the various grains. The sample contains 36 grains with an average grain size of 6 nm. The periodicity along the [110] axis common to all grains is kept at the lattice periodicity along that direction. The grain boundaries present in these samples are of pure tilt character and have random misorientation angles. After their initial creation, the samples were fully relaxed using a conjugate gradient technique. The initial relaxation included the simultaneous energy minimization with respect to the total sample volume. The relaxed configuration is then used as a starting configuration in both the molecular

statics and the dynamics techniques to study crack propagation using the same EAM interatomic potential and cyclic loading.

**Results.**—The samples were subject to cyclic loading with an average stress intensity,  $K_{ave}$  of  $0.96 \text{ MPa}\sqrt{\text{m}}$ . Four values of the stress intensity amplitude were considered, namely, 1.28, 1.6, 1.76, and  $2.9 \text{ MPa}\sqrt{\text{m}}$ . For the molecular dynamics simulations 2000 MD steps per cycle were used with a time step of  $1 \times 10^{-15} \text{ s}$  and a temperature of 300 K. Simulations using molecular statics were also carried out where the crack is allowed to reach a local equilibrium configuration at both the low and the high loading points of the cycle. These simulations are therefore representative of low cycle fatigue where the system has enough time to reach equilibrium as the cycle proceeds. Most importantly, the comparison of these two techniques gives an assessment of the importance of the fast time scale in the MD simulations in the mechanisms observed and in the rates of crack advance. The simulations reported here follow the crack using this technique for 30 cycles. The threshold stress intensity amplitude observed is about 1 to  $1.1 \text{ MPa}\sqrt{\text{m}}$ .

Crack advance is shown in Fig. 1, where the position of the crack tip is plotted as a function of the number of cycles. The slopes in this type of plot were computed for each of the stress intensity amplitudes considered. Figure 2 shows the resulting rates of crack advance calculated using molecular dynamics for the three values of the stress intensity amplitude. The figure also shows the results of molecular statics and the available experimental data for nanocrystalline Ni by Hanlon, Kwon, and Suresh [10].

The results show that crack advance rates are not very sensitive to the technique with molecular dynamics and molecular statics giving similar results. This suggests that the molecular dynamics results do not have major spurious effects due to the unrealistically high loading rates. To further establish confidence in these results, we studied the basic mechanisms of crack advance using both techniques. For both cases, we see a continuous increase in the number of dislocations present in the crack tip region as the crack advances, and the formation of nanovoids or vacancy

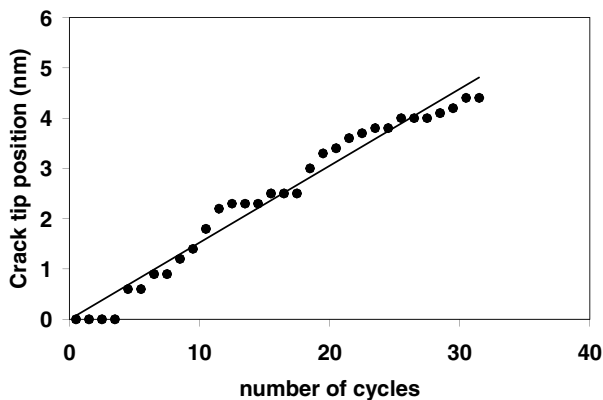


FIG. 1. Crack advance as a function of the number of cycles observed in a static simulation with  $\Delta K = 1.28 \text{ MPa}\sqrt{\text{m}}$ .

clusters ahead of the main crack. Figure 3 shows the number of dislocations and nanovoids observed as the cyclic deformation proceeds. Figure 4 shows crack tip configurations corresponding to cycles 1, 12, and 20. The simulations shown in Figs. 3 and 4 were conducted using molecular statics at a stress intensity amplitude of  $1.28 \text{ MPa}\sqrt{\text{m}}$ . Frames on the left side of Fig. 4 are for maximum loading conditions, whereas frames on the right show the minimum loading configurations. The visualization in Fig. 4 is carried out using the local hydrostatic stress calculated for each atom. The gray scale shows areas under tension as light gray and areas under compression in darker shades. The visualization technique requires an assumption regarding the local atomic volume for each atom, which we considered constant. The technique allows the visualization of the damage, including stacking faults that are the result of the emission of partial dislocations from the grain boundaries.

In Fig. 5 we show greater detail of the configuration of the tip as the crack is loaded to the maximum stress intensity after 26 and 31 cycles. The main mechanism of crack advance is the formation of vacancy clusters ahead of the crack tip that result from the plastic deformation in the tip region. The results in this figure are obtained using a static technique where the crack reached local equilibrium at both the high and the low loading points of each cycle. The results obtained using molecular dynamics are similar in nature, also showing the formation of nanovoids ahead of the main crack. This mechanism of the crack advance was also observed in the monotonic fracture simulation studies of Ni that we carried out previously [8]. We note that crack advance and the formation of the nanovoids under monotonic loading occurred at stress intensity amplitudes that are 2 to 3 times higher than those used here as the maximum loading. The formation of nanovoids in a grain boundary ahead of the main crack seems to be a general failure mechanism in nanocrystalline materials. In the present simulations we find that these nanovoids are created by the presence of dislocations emitted from the

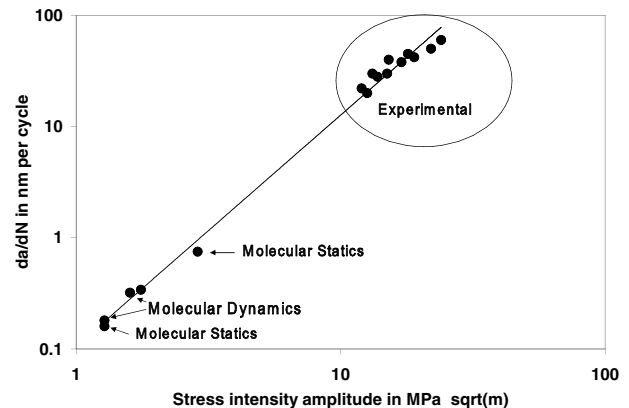


FIG. 2. Rate of crack advance for both molecular statics and dynamics simulations together with experimental results by Hanlon, Kwon, and Suresh [10].

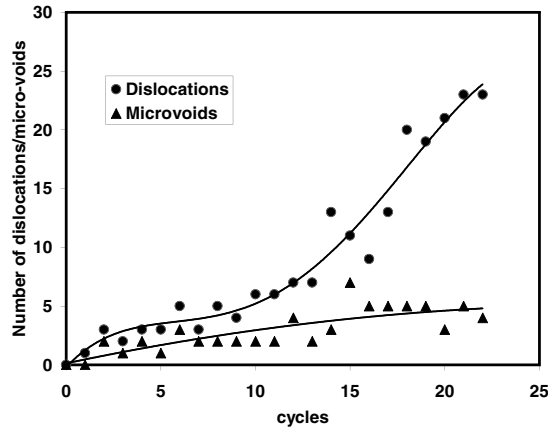


FIG. 3. The number of dislocations and nanovoids present in the crack tip region as the cyclic loading proceeds.

crack tip. In Fig. 5 we can see nanovoids both within the grain where the crack tip is located and at the grain boundary. The nanovoids within the grain are related to the presence of two or more dislocations in adjacent planes. The arrival of the dislocations to the grain boundary region also causes the formation of nanovoids, when the dislocations cannot cross into the adjacent grain. We observe a distribution of these nanovoids that is essentially confined to the grain where the crack tip is located, with most of the dislocations being unable to continue to glide across the grain boundaries.

It is encouraging to note that our results yield four points in the curve of crack advance versus stress intensity amplitude that are very consistent with the experimental

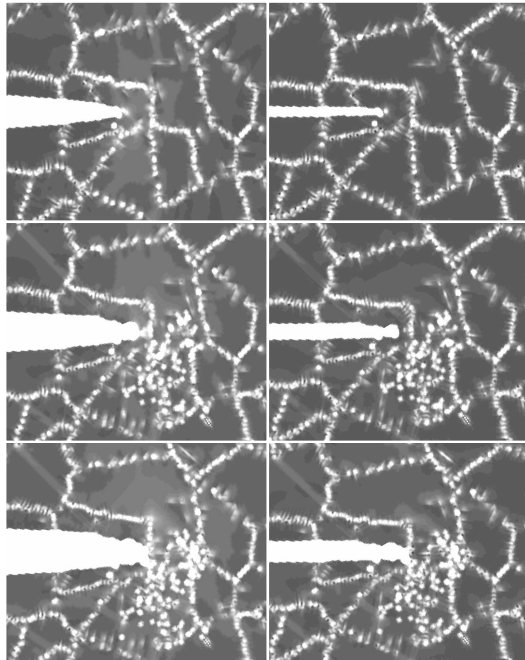


FIG. 4. Crack tip configurations for cycles 1, 12, and 20. Molecular statics with  $\Delta K = 1.28 \text{ MPa}/\sqrt{\text{m}}$ . Left frames are for maximum loading and right frames for minimum loading.

measurements in nanocrystalline Ni. The results shown in Fig. 2 show that our simulations are in the Paris regime. This can be related to the small size scale of the microstructural features in our sample. The size of our cyclic plastic zone is comparable to the grain size, as shown in Fig. 4, the point where a transition to a Paris regime typically occurs [11]. Our results imply a Paris law exponent of about 2, indicated by the line in Fig. 2. This exponent is expected from deformation controlled geometrical models that are based on crack tip opening displacement which is related to the square of the stress intensity amplitude [11]. We can analyze in more detail our results in the light of models that have been proposed for a Paris law exponent of 2. One model is described by Weertman [12] for fatigue crack growth controlled by crack tip blunting. In this model, the crack growth rate is given by  $da/dN = b(\Delta K/2gK_c)^2$  (Eq. 10.37 in Ref. [12]), where  $da/dN$  is the crack growth rate per cycle,  $b$  is the Burgers vector,  $g$  is the ratio between critical stress intensity factors for dislocation emission and cleavage, and  $K_c$  is the critical stress intensity for cleavage. Using a value of 0.9 for the ratio  $g$ , the Burgers vector of a Shockley partial dislocation of 0.144 nm and a value of 0.96  $\text{MPa}\sqrt{\text{m}}$  for  $K_c$  we obtain  $da/dN = 0.087\Delta K^2$ , with  $da/dN$  in nm per cycle and the stress intensity in  $\text{MPa}\sqrt{\text{m}}$ . This compares well with the best fit line obtained from our four data points which is  $da/dN = 0.095\Delta K^2$  in the same units. This good agreement suggests that the crack advance process observed here is controlled by crack tip blunting caused by dislocation emission. Alternatively, one can use a simpler formulation also described by Weertman [13] for a similar model which gives  $da/dN$  of the order of  $(\Delta K/G)^2$ . This for Ni would imply  $da/dN = 0.173\Delta K^2$  in the same units, which is again of the order of our best fit values. The models that give  $da/dN$  of the order of  $(\Delta K/\sigma_{\text{yield}})^2$  or  $\Delta K^2/G \times \sigma_{\text{yield}}$  would significantly overestimate the current results. To further support our conclusion that the crack advance is controlled by blunting caused by dislocation emission, Fig. 6 shows a plot of the crack tip position versus the total cumulative blunting caused by dislocation emission. The total cumulative blunting values in this figure were obtained from the total number of dislocations observed in the sample, multiplying by the

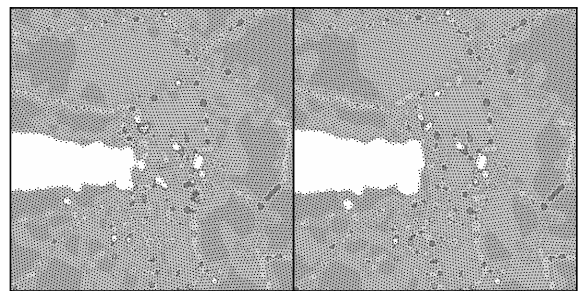


FIG. 5. Crack tip configurations for 26 (left) and 31 (right) cycles. Molecular statics with  $\Delta K = 1.28 \text{ MPa}/\sqrt{\text{m}}$ . Frames show maximum loading.

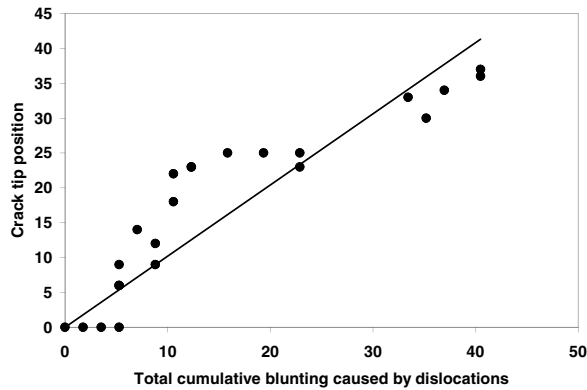


FIG. 6. Crack tip position plotted as a function of the total cumulative blunting caused by dislocation emission.

projected Burgers vector. We assume that all dislocations emitted from the crack tip caused blunting of the crack. The data in Fig. 6 indicate that the total crack advance is of the order of the total cumulative blunting that can be attributed to the dislocations observed in the sample.

Regarding the threshold stress, the values we obtained (about  $1 \text{ MPa}\sqrt{\text{m}}$ ) also compare very well with the model estimate of  $Gb^{1/2}$  [13] which gives  $0.91 \text{ MPa}\sqrt{\text{m}}$ . The threshold value found here also is of the order of the estimates based on dislocation dynamics models [3–6] of  $3 \times 10^{-6} E\sqrt{m}$ , which for a value of the Young modulus  $E$  of 200 GPa gives  $0.6 \text{ MPa}\sqrt{\text{m}}$ . For stress intensity amplitudes just above the threshold value we obtain crack advance rates that are of the order of an interatomic distance, consistent with the analysis given by Weertman [13].

Although we see evidence of damage accumulation in the sample, as shown in Fig. 4, the predicted Paris law exponent based on damage accumulation models is 4 [11] which does not agree with our results. This can be related to the presence of grain boundary material in the immediate vicinity of the source of dislocation emission. For the nanocrystalline materials studied here, the dislocations that are emitted from the crack tip interact with the grain boundaries present in the crack tip zone at very short distances from where they are emitted. Typically, many dislocations travel to a nearby grain boundary and are then absorbed. The grain boundaries themselves contribute to the accommodation plasticity, as has been shown in many studies of deformation of nanocrystalline materials [1]. The models based on damage accumulation are based on calculations of the field of a distribution of dislocations, as in the model by Weertman [14], or on a calculation of the energy balance necessary for crack advance, as in the model by Rice [15]. The particularities related to the very small grain sizes and large fraction of grain boundaries of the nanocrystalline materials discussed above are not taken into account. The very small grain sizes also

promote a more homogeneous distribution of the damage, as discussed by Misra and co-workers [16].

In summary, these first atomistic studies of fatigue behavior in nanocrystalline materials show a Paris exponent of two and a mechanism that is dominated by the role of the dislocations emitted from the crack tip, with a crack advance that is of the order of the blunting caused by the emitted dislocations. Our results are consistent with experimental measurements of crack advance rates [10]. Regarding the mechanisms of crack advance, nanovoids created during the deformation process were found, in agreement with simulations and experimental transmission electron microscopy results obtained for monotonic fracture [1].

This work was supported by AFOSR, Metallic Materials Program. The authors acknowledge critical discussions with Alan Needleman, Brown University.

---

\*Electronic address: diana@vt.edu

- [1] K. S. Kumar, H. Van Swygenhoven, and S. Suresh, *Acta Mater.* **51**, 5743 (2003).
- [2] J.R. Weertman, D. Farkas, K. Hemker, H. Kung, M. Mayo, R. Mitra, and H. Van Swygenhoven, *MRS Bull.* **24**, 44 (1999).
- [3] V. S. Deshpande, A. Needleman, and E. Van der Giessen, *Acta Mater.* **51**, 4637 (2003).
- [4] V. S. Deshpande, A. Needleman, and E. Van der Giessen, *Acta Mater.* **51**, 1 (2003).
- [5] V. S. Deshpande, A. Needleman, and E. Van der Giessen, *Acta Mater.* **50**, 831 (2002).
- [6] V. S. Deshpande, A. Needleman, and E. Van der Giessen, *Acta Mater.* **49**, 3189 (2001).
- [7] Y. Mishin, D. Farkas, M.J. Mehl, and D. A. Papaconstantopoulos, *Phys. Rev. B* **59**, 3393 (1999).
- [8] D. Farkas, H. Van Swygenhoven, and P.M. Derlet, *Phys. Rev. B* **66**, 060101 (2002).
- [9] H. Van Swygenhoven, D. Farkas, and A. Caro, *Phys. Rev. B* **62**, 831 (2000).
- [10] T. Hanlon, Y.N. Kwon, and S. Suresh, *Scr. Mater.* **49**, 675 (2003).
- [11] S. Suresh, *Fatigue of Materials* (Cambridge University Press, Cambridge, England, 1998), 2nd ed.
- [12] J. Weertman, *Dislocation Based Fracture Mechanics* (World Scientific Publishing, Singapore, 1996).
- [13] J. Weertman, in *High Cycle Fatigue of Structural Materials*, edited by W.O. Soboyejo and T.S. Srivatsan (The Minerals, Metals and Materials Society (TMS) of the AIME, Warrendale, PA, 1997), pp. 41–48.
- [14] J. Weertman, *Int. J. Fract. Mech.* **2**, 460 (1966).
- [15] J.R. Rice, in *Fatigue Crack Propagation* (ASTM, Philadelphia, 1967), Vol. 415, p. 247.
- [16] A. Misra, H. Kung, D. Hammon, R.G. Hoagland, and M. Nastasi, *Int. J. Damage Mech.* **12**, 365 (2003).